Localization and rearrangement modulation of the N-terminal arm of the membrane-bound major coat protein of bacteriophage M13

ARTICLE *in* BIOCHIMICA ET BIOPHYSICA ACTA · JANUARY 2001

Impact Factor: 4.66 · DOI: 10.1016/S0005-2736(00)00314-X · Source: PubMed

4 AUTHORS, INCLUDING:

Ruud B Spruijt
Wageningen University
91 PUBLICATIONS **1,129** CITATIONS

SEE PROFILE

ELSEVIER

Biochimica et Biophysica Acta 1509 (2000) 311–323

BIOCHIMICA ET BIOPHYSICA ACTA
BBA

www.elsevier.com/locate/bba

Localization and rearrangement modulation of the N-terminal arm of the membrane-bound major coat protein of bacteriophage M13

Ruud B. Spruijt *, Alexander B. Meijer, Cor J.A.M. Wolfs, Marcus A. Hemminga

Wageningen University and Research Center, Department of Biomolecular Sciences, Laboratory of Molecular Physics, Dreijenlaan 3, 6703 HA Wageningen, The Netherlands

Received 9 June 2000; received in revised form 14 August 2000; accepted 17 August 2000

Abstract

During infection the major coat protein of the filamentous bacteriophage M13 is in the cytoplasmic membrane of the host *Escherichia coli*. This study focuses on the configurational properties of the N-terminal part of the coat protein in the membrane-bound state. For this purpose X-Cys substitutions are generated at coat protein positions 3, 7, 9, 10, 11, 12, 13, 14, 15, 17, 19, 21, 22, 23 and 24, covering the N-terminal protein part. All coat protein mutants used are successfully produced in mg quantities by overexpression in *E. coli*. Mutant coat proteins are labeled and reconstituted into mixed bilayers of phospholipids. Information about the polarity of the local environment around the labeled sites is deduced from the wavelength of maximum emission using AEDANS attached to the SH groups of the cysteines as a fluorescent probe. Additional information is obtained by determining the accessibility of the fluorescence quenchers acrylamide and 5-doxyl stearic acid. By employing uniform coat protein surroundings provided by TFE and SDS, local effects of the backbone of the coat proteins or polarity of the residues could be excluded. Our data suggest that at a lipid to protein ratio around 100, the N-terminal arm of the protein gradually enters the membrane from residue 3 towards residue 19. The hinge region (residues 17–24), connecting the helical parts of the coat protein, is found to be more embedded in the membrane. Substitution of one or more of the membrane-anchoring amino acid residues lysine 8, phenylalanine 11 and leucine 14, results in a rearrangement of the N-terminal protein part into a more extended conformation. The N-terminal arm can also be forced in this conformation by allowing less space per coat protein at the membrane surface by decreasing the lipid to protein ratio. The influence of the phospholipid headgroup composition on the rearrangement of the N-terminal part of the protein is found to be negligible within the range thought to be relevant in vivo. From our experiments we conclude that membrane-anchoring and space-limiting effects are key factors for the structural rearrangement of the N-terminal protein part of the coat protein in the membrane.

Keywords: Fluorescence spectroscopy; Cysteine scanning; M13 major coat protein; N-terminal protein arm rearrangement; Lipid–protein interaction; Phage assembly

Abbreviations: IAEDANS, *N*-(iodoacetylaminoethyl)-5-naphthylamine-1-sulfonic acid; DOPC, dioleoyl phosphatidylcholine; DOPG, dioleoyl phosphatidylglycerol; DOPE, dioleoyl phosphatidylethanolamine; HPSEC, high-performance size-exclusion chromatography; RPC, reverse-phase chromatography; IPTG, isopropylthio-β-D-galactoside; SDS, sodium dodecyl sulfate; TFE, trifluoroethanol; DTT, dithiothreitol; TEA, triethylamine; PAGE, polyacrylamide gel electrophoresis; CL, cardiolipin; K_{sv}, Stern–Volmer constant; F, fluorescence intensity in the presence of quencher; F_0, fluorescence intensity in the absence of quencher; L/P, lipid to protein molar ratio; TBS, Tris-buffered saline

* Corresponding author. Fax: +31-317-482725; E-mail: ruud.spruijt@virus.mf.wau.nl

0005-2736/00/$ – see front matter
PII: S0005-2736(00)00314-X

1. Introduction

In the filamentous bacteriophage M13 a large number of copies of the major coat protein forms a cylindrical coat around the circular, single-stranded DNA genome. During infection, the major coat protein (the product of gene VIII) is involved in various environmental and structural rearrangements. First there are the processes of phage disassembly and subsequent deposition of the coat protein into the *Escherichia coli* inner membrane. These processes are followed by the biosynthesis of the procoat, the membrane insertion and subsequent removal of the signal sequence by the host cell leader peptidase. Finally the protein takes part in the complex process of cooperative assembly and phage-extrusion [1–4]. To accomplish all these different functions of the coat protein, the primary sequence must be such to enable sufficient functioning in all processes, which of course not necessarily imply optimal functioning with respect to one specific aspect. In this sense, a proper functioning of the coat protein will generally be achieved by adapting its secondary and tertiary structure.

Much is known about the aggregational behavior and overall secondary structure of the coat protein embedded in phospholipid bilayers [5–8]. The primary and secondary structure of the coat protein are depicted in Fig. 1. New insights about the conformation mainly originate from experiments performed on the coat protein solubilized in detergents as membrane-mimicking systems. Detailed secondary structure determination as performed on the coat protein solubilized in sodium dodecyl sulfate (SDS) or dodecyl phosphatidylcholine micelles clearly shows an α-helix ranging from residues 25 up to 45 [9,10]. This finding is in agreement with the result of a cysteine-scanning study on the putative transmembrane domain performed on the coat protein reconstituted in phospholipid bilayers [11,12], and appeared to be shifted from the predicted transmembrane domain [13,14]. In the N-terminal part of the coat protein a short amphipathic α-helical structure (residues 7–16) has been established, with residues demonstrating considerable motion on the nanosecond and picosecond time scales. Furthermore, a motion of the amphipathic helical arm with respect to the transmembrane helix has been proposed [15]. The hinge region, connecting the two helices, exhibits α-helical, turn-like features as well as additional flexibility of its residues [9,10].

Between the amphipathic N-terminal helix and the transmembrane helix of the membrane-bound coat protein an angle of approximately 90° is found [16–18]. This L-shape implies that the N-terminal helix lies in the plane of the membrane. However, when the coat protein is part of the M13 phage particle, it is arranged in one continuous, slightly bent helix [19,20]. No information is available about what factors direct the rearrangement of the two helices in the viral and membrane-bound states of the coat protein, as will take place during the phage assembly process. However, an extended N-terminal protein part could well be a structural and functional intermediate of the membrane-bound coat protein in various stages of the viral replication process.

In the present study we follow a site-specific probing approach for the N-terminal part, similar as has

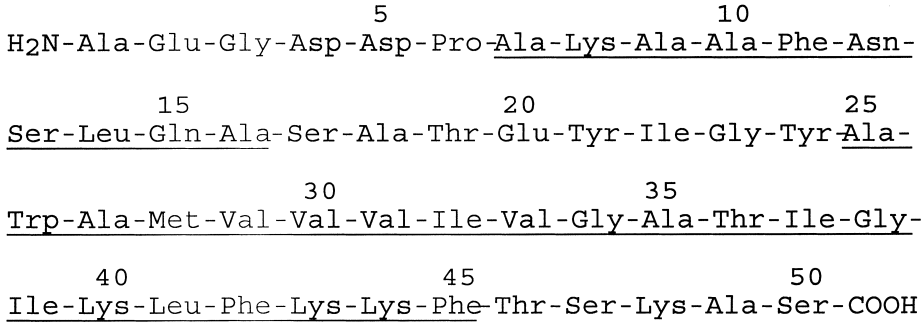

Fig. 1. The primary and secondary structure of the mature part of the major coat protein of bacteriophage M13. The amphipathic α-helix and the transmembrane α-helix are underlined. The part of the protein connecting the two helical domains is called the hinge region.

been carried out for the C-terminal part of the M13 major coat protein [11], and recently for the Pf3 major coat protein [21]. The cysteine-scanning method is a suitable technique to obtain information about the local polarity of the probe, which can be related to the membrane-embedment of the protein. The method has been described for various membrane proteins [12,22–24]. We prepared a number of coat protein mutants containing unique cysteine residues at specific positions along the N-terminal amino acid sequence. The cysteine residues were specifically labeled with the fluorescent environmental probe *N*-(iodoacetylaminoethyl)-5-naphthylamine-1-sulfonic acid (AEDANS). The fluorescence properties and accessibilities towards various quencher molecules are reported to be dependent on polarity as well as steric effects [25,26]. By employing uniform coat protein surroundings provided by an organic solvent (TFE) or a micellar system (SDS), local effects of the backbone of the coat proteins or polarity of the residues could be excluded. Based on a fixed labeling position, additional substitutions of various N-terminal amino acid residues in double protein mutants elucidate the importance of these residues in affecting the association of the N-terminal protein arm to the membrane. Phospholipid composition and lipid to protein ratio are further tested as possibly involved in the membrane-binding behavior of this protein domain.

2. Materials and methods

2.1. Cloning procedures

Both the mature coat protein part of bacteriophage M13 gene VIII (without the leader sequence) and the complete bacteriophage M13 gene VIII (including the leader sequence) were obtained by the polymerase chain reaction (PCR) using M13 mp18 RF DNA as template and primers based on the sequence as determined by Van Wezenbeek [27]. Oligonucleotide primers (Amersham Pharmacia Biotech) were designed to add a NdeI restriction site upstream of the start codon (5′-GGGCATATGGCTGAGGGTGACGAT for the mature coat protein part of the gene, and 5′-GGGCATATGAAAAAGTCTTTAGTCCT for the complete gene VIII) and a *Bam*HI restriction site downstream of the stop codon (5′-CCCGGATCCTCAGCTTGCTTTCGAGG for both reactions). The PCR amplified fragments were purified by polyacrylamide gel electrophoresis. After digestion with *Nde*I and *Bam*HI they were cloned into the respective sites of a pT7-7 expression vector [28]. *E. coli* strain DH5αF′ was used for the cloning vector.

2.2. Preparation of cysteine-containing major coat protein mutants

The QuikChange site directed mutagenesis procedure (Stratagene) was used to introduce unique cysteine residues at various positions along the primary structure of the major coat protein. The procedure was also used for other modifications of the coat protein. For each modification two complementary synthetic oligonucleotide primers (Amersham Pharmacia Biotech) were designed, and used together with the double stranded pT7-7 expression vector (containing the cloned M13 gene VIII) as a template. Following temperature cycling and the selection for mutated DNA by DpnI digestion, the expression vectors were transformed into supercompetent cells of *E. coli* XL1-Blue. Plasmid DNA was isolated using the Wizard DNA purification system (Promega) and used for transformation into competent cells of *E. coli* BL21 (DE3) [29]. Transformed cells were incubated in LB medium (1% (w/v) select peptone, 0.5% (w/v) yeast extract, 1% (w/v) NaCl) to allow expression of ampicillin resistance, and grown overnight on LB-agar in the presence of 0.01% (w/v) ampicillin (Boehringer). Plasmid DNA, isolated from a liquid culture as mentioned before, was used for automated DNA sequencing. Ready-to-use inoculates were prepared in the presence of glycerol (22% w/w, final concentration) and stored at −70°C.

2.3. Expression of modified M13 gene VIII and identification of the gene product

Cells of *E. coli* BL21 (DE3) containing pT7-7 (gene VIII mutant) were grown at 37°C in LB medium supplemented with 0.2% (w/v) glucose and 0.01% (w/v) ampicillin. The optical density at 600 nm of the culture was monitored and at an $OD_{600\,nm}$ of about 0.6 the expression of the target

gene was induced by adding IPTG up to 0.15 mM final concentration. Aliquots (25 μl) were taken before induction and after different times of incubation after induction, and checked for the presence of the gene product using Tricine SDS–polyacrylamide gel electrophoresis, as described [30]. Western blotting [31] and immunodetection were performed using anti-rabbit IgG conjugated with alkaline phosphatase (Boehringer). Primary antibodies against the major coat protein of bacteriophage M13 were raised in female New Zealand White rabbits using highly purified biosynthetic major coat protein as obtained from the phenol extraction procedure described previously [32]. The serum exclusively reacted with the major coat protein applied to the gel and not with proteins of host *E. coli* BL21 (DE3).

2.4. Expression, labeling and purification of modified M13 major coat proteins

E. coli BL21 (DE3) containing the respective pT7-7 plasmids were grown in 8-l cultures as described before. Cells were harvested by centrifugation (10 min at $7000 \times g$) within 45–90 min after induction. The cells were resuspended in TBS/DTT (Tris-buffered saline/dithiothreitol) buffer (25 mM Tris–HCl (pH 7.5), 137 mM NaCl, 2.7 mM KCl, 1 mM DTT) and stored at −20°C. The total membrane fraction was isolated after cell lysis by sonication (Branson B15 sonifier, 5 min, 90 W output, 50% pulse, on ice) and subsequent centrifugation (30 min $45\,000 \times g$ at 4°C). The pelleted membrane fraction was resuspended in TBS/DTT buffer by brief sonication. Amounts of cellular material out of 2 l cell culture were used for further treatment. Prior to reverse-phase chromatography (RPC) the major coat protein was extracted from the total membrane fraction. Equal volumes of resuspended total membrane fraction and trifluoroethanol (TFE) were thoroughly mixed for 1 min and non-extractable material was removed by centrifugation (5 min $10\,000 \times g$). The clear membrane extract in the supernatant was immediately applied on a Source 15RPC HR10/10 column (Amersham Pharmacia Biotech), and eluted with water (flow 1.0 ml/min) using a Pharmacia-LKB Ultrochrom GTi Bioseparation system. After elution of all non-binding material (as monitored at 280 nm) the major coat protein was eluted using a steep linear gradient of mixtures of solvent A: pure water and solvent B: isopropanol/0.2% (v/v) triethylamine (TEA). Starting at 0% (v/v), solvent B increased with a rate of 5%/min up to 100%, and decreased with a rate of 10%/min back to 0% of solvent B. Fractions were collected and analyzed by Tricine SDS–PAGE. For the purpose of labeling with IAEDANS (purchased from Molecular Probes), the fractions containing the major coat protein were pooled and mixed with TFE to achieve optimal accessibility conditions. After the pH was adjusted to approx. 8 by addition of a small amount of TEA, an estimated small molar excess of IAEDANS was added and the mixture was stirred in the dark at room temperature for 3 h. The reaction was stopped by addition of an excess of β-mercaptoethanol. Solid sodium cholate (Sigma) was added up to 500 mM and dissolved completely before the reaction mixture was applied on a preparative HiLoad Superdex 75 prepgrade column (2.6×60.0 cm) (Amersham Pharmacia Biotech). This column was eluted with 50 mM sodium cholate, 10 mM Tris–HCl (pH 8.0), 0.2 mM EDTA, 150 mM NaCl at a flow of 2 ml/min to separate the labeled coat protein from accompanying proteins and excess unbound AEDANS. Fractions containing the AEDANS-labeled coat protein, as monitored by a linear fluorescence detector (excitation wavelength set at 340 nm, emission wavelength set at 480 nm) were pooled and concentrated using ultrafiltration over an Amicon YM3 membrane. The AEDANS-labeled coat protein fractions were checked for purity and protein content by Tricine SDS–PAGE. Wild-type major coat protein as well as mutant coat proteins with a cysteine at positions 25 and 46 were obtained, labeled with IAEDANS and purified as described before [11].

2.5. Reconstitution of the AEDANS-labeled coat protein into phospholipid bilayers

Unless stated otherwise, reconstitution of the labeled coat protein mutants into dioleoyl phosphatidylcholine (DOPC) and dioleoyl phosphatidylglycerol (DOPG) vesicles (both lipids obtained from Sigma) in a 80/20% (mol/mol) ratio was performed in the dark using the cholate-dialysis procedure as described earlier [32]. The final molar lipid to protein ratio was 100. The resulting proteoliposomes in 10

mM Tris–HCl (pH 8.0), 0.2 mM EDTA, 150 mM NaCl were directly used for fluorescence and circular dichroism measurements.

2.6. Circular dichroism measurements

Circular dichroism spectra were recorded from 200 to 260 nm on a JASCO 715 spectrometer at room temperature, using a 1-mm path length cell, 1 nm bandwidth, 0.1 nm resolution and 1 s response time. Spectra were corrected for the background and protein content.

2.7. Steady-state fluorescence measurements

The fluorescence properties of the AEDANS-labeled major coat protein, reconstituted into DOPC/DOPG bilayers, were recorded at room temperature on a Perkin–Elmer LS-5 luminescence spectrophotometer. The excitation wavelength was 340 nm and emission scans were recorded from 470 to 530 nm. Excitation and emission slits were set at 5 nm. The concentration of labeled coat protein was kept constant at 2.5 or 5 μM and is mentioned in the tables and figure legends. The optical density at the excitation wavelength never exceeded 0.1. Fluorescence intensities were corrected for background by subtracting the spectrum of unlabeled wild-type major coat protein, reconstituted into the same phospholipid bilayers, and recorded under the same conditions. Due to a different instrumental set-up of the luminescence spectrophotometer the wavelength of maximum emission intensity showed an 8 nm red shift as compared to the results reported earlier [11]. To enable comparison two major coat protein mutants, labeled to a unique cysteine at positions 25 and 46, were included in all experiments. The variations of the measured wavelengths of maximum emission are always found to be within 1 nm.

Steady-state quenching studies were performed by addition of various amounts of a 2.67 M acrylamide solution (Merck, electrophoresis quality) to a final concentration of 242 mM. Alternatively 5-doxyl stearic acid (Aldrich Chemical Co.) was added from a 12.5 mM solution to a fixed final overall concentration of 0.2 mM. Emission spectra were recorded 1 min after each addition and the stable fluorescence intensities were corrected for background and dilution. Variations of the calculated K_{sv} and F_0/F values are usually within 5%.

3. Results

3.1. Expression of the target gene and identification of the gene product

Since no coat protein mutants containing a cysteine residue in the N-terminal protein part could be generated resulting in the appearance of viable bacteriophages, as has been employed earlier [11], we have cloned the coat protein gene into the pT7-7 expression vector. As a consequence, the control for proper functioning of the coat protein by phage viability is lacking. Moreover, the target protein now needs to be purified from the host cell, requiring excessive and complicated purification protocols. The expression of the target gene results in a reduced cell growth and even a decrease in optical density of the cell culture after prolonged times. As the synthesis of the gene product is accompanied by membrane insertion, high amounts of the coat protein appear to be toxic and will finally result in cell lysis. Attempts were made to direct the synthesized coat protein into the cell cytoplasm by removal of the leader sequence of the coat protein (the first 23 amino acids coded by gene VIII). However, no mature coat protein could be detected, even not by employing immunodetection. Therefore, it is essential to apply the complete gene VIII (including the leader sequence) for coat protein synthesis. Also, fusion to a water-soluble protein appeared not to be an alternative as was demonstrated for the closely related M13 minor coat proteins, which were still found preferentially present in the *E. coli* inner membrane [33].

Neither decreasing the growth temperature nor lowering the level of expression (by lowering the final IPTG concentration) did result in a higher yield. To obtain appropriate amounts of coat protein, large volumes of growing culture were required. Moreover, cell growth is only allowed for quite a short time (within 45–90 min) after the induction of coat protein synthesis. In the case of prolonged growing times after induction of the target gene expression, an ad-

ditional small band of a larger protein is detected by the Tricine SDS–PAGE and subsequent immunodetection. This band is identified to contain M13 procoat based on recognition by the antiserum, which is raised against the mature part of the gene VIII product. The protein also migrated identically on gel as compared to the procoat mutant (gene VIII S-3F), which was characterized by a strongly decreased processing rate by leader peptidase [34]. The appearance of the procoat after prolonged incubation times is indicative for defects in the processing by leader peptidase, because the cell integrity or functioning is distorted.

To localize the coat protein after expression, cells were fractionated according to Russel and Kazmierczak [35] and subjected to gel electrophoresis. The coat protein is predominantly found in the fraction containing the inner or cytoplasmic membranes (data not shown).

X-Cys substitutions are generated at coat protein positions 3, 7, 9, 10, 11, 12, 13, 14, 15, 17, 19, 21, 22, 23, and 24, covering the entire N-terminal part of the M13 major coat protein (see Fig. 1). All coat protein mutants, in which an amino acid residue has been substituted for a cysteine residue, are obtained in amounts comparable to that of wild-type coat protein, i.e., mg quantities. However, severe additional modifications (Table 1) occasionally resulted in lower amounts of coat protein.

3.2. Purification and labeling of the coat protein mutants

A combined protein labeling and purification protocol was developed. Organic solvents are applied to enable RPC and to serve optimal labeling conditions. After achieving a major purification effect by RPC, care has to be taken in proper solubilizing the coat protein by detergents. After harvesting the cells by centrifugation and the preparation of the membrane fraction, almost all mature coat protein (but not the unprocessed procoat; data not shown) is successfully extracted using the organic solvent TFE and subsequently purified on a Source 15RPC HR10/10 column. The pooled major coat protein containing fractions are diluted with TFE to prevent protein–protein interactions, and to achieve an optimal accessibility of the cysteines thiol group for the fluorescent probe AEDANS to be attached. The AEDANS-labeled coat protein is further purified from other cellular impurities and excess free label, using high performance size exclusion chromatography (HPSEC). For this purpose, it is essential to add a huge excess of the detergent sodium cholate to get an appropriate solubilization of the coat protein. The final isolates of labeled coat protein are applied to Tricine SDS–PAGE to check the purity and the yield of coat protein. Typically 0.5–1 mg of labeled mutant coat protein is obtained per liter cell culture. The

Table 1
Quencher efficiencies and environmental polarity of various AEDANS-labeled M13 major coat protein A7C-derived double mutants in DOPC/DOPG membranes

M13 coat protein mutant	Emission maximum K_{sv} (nm)[a]	Quenching by acrylamide (M^{-1})[a]	Quenching by 5-doxyl stearic acid F/F_0
A7C	495	2.99	0.54
A7C/K8A	499	3.85	0.63
A7C/A10I	492	2.62	0.48
A7C/F11A	502	5.18	0.71
A7C/L14A	502	5.37	0.81
A7C/F11A/L14A	505	5.98	0.83
A7C/L14D	502	5.07	0.70

Wavelengths of maximum emission and accessibilities to the hydrophilic quencher acrylamide and hydrophobic quencher 5-doxyl stearic acid are determined on AEDANS, attached to various M13 coat protein mutants at cysteine position 7. The coat protein at a final concentration of 2.5 μM is reconstituted into DOPC/DOPG at L/P 100. The concentrations of the quencher molecules are given in Section 2.

[a]Emission maxima and quenching efficiencies of these double mutants when brought in a homogeneous environment provided by TFE were equal and constant at 498 nm and $F/F_0 = 1.25$, respectively.

purity is found to exceed at least 95%, as is judged from stained protein bands on gel. Circular dichroism spectra of mutant protein, containing the mutation L14A or A10I, reconstituted into phospholipid, were found to be identical to that of reconstituted wild-type coat protein (data not shown).

3.3. Environmental polarity probing approach in a uniform protein surrounding

The spectral properties of AEDANS provide local environmental information concerning the extent of membrane penetration [11,25,36]. To check whether also the protein itself affects the fluorescence results, the coat protein was brought into a homogeneous environment. For these experiments we used 85% (v/v) TFE in water, and the strong cationic detergent SDS. The wavelengths of maximum emission of the attached AEDANS probes at the different N-terminal positions and the transmembrane boundary positions (25 and 46) are given in Fig. 2A. The wavelengths of maximum emission of the coat protein mutants dissolved in 85% (v/v) TFE in water are almost constant at a value of 498 nm, with only small variations (within 3 nm) at position 3 and position 25: 501 and 495 nm, respectively. It should be noted that the wavelength of maximum emission of unbound AEDANS (represented as amino acid residue number 0) is also 498 nm. Similar results are obtained in SDS, showing a higher average wavelength of maximum emission at 508 nm, and again small variations within 4 nm. The wavelength of maximum emission of the unbound AEDANS solubilized by SDS is slightly higher at 513 nm (see Fig. 2A; unbound AEDANS is represented again on position 0).

Since it is known that the accessibility of a fluorophore to a quencher depends upon the polarity and steric effects [26,37,38], the quenching efficiency can also provide information about the local surrounding. The reduced fluorescence intensities, due to the presence of the quencher molecule acrylamide (125 mM final concentration), as a function of the different AEDANS attachment sites on the coat protein, are given in Fig. 2B. Although the quenching efficiency in SDS is twice as much as that found in TFE, only small differences in quenching efficiency between the various coat protein mutants are found in TFE and SDS. Moreover, the wavelengths of maximum emission of the AEDANS probes attached to the different positions along the coat proteins primary structure hardly shift upon addition of the hydrophilic quencher acrylamide (data not shown), indicating again a homogeneous environment. These experiments underline the uniformity of the local environment of the N-terminal part of the coat protein provided by these two media, and greatly reduces the local environmental influence of the coat protein itself. Therefore, the local amino acid effect on the optical properties of the probe can be neglected in the following experiments, where the environment is imposed by a phospholipid bilayer.

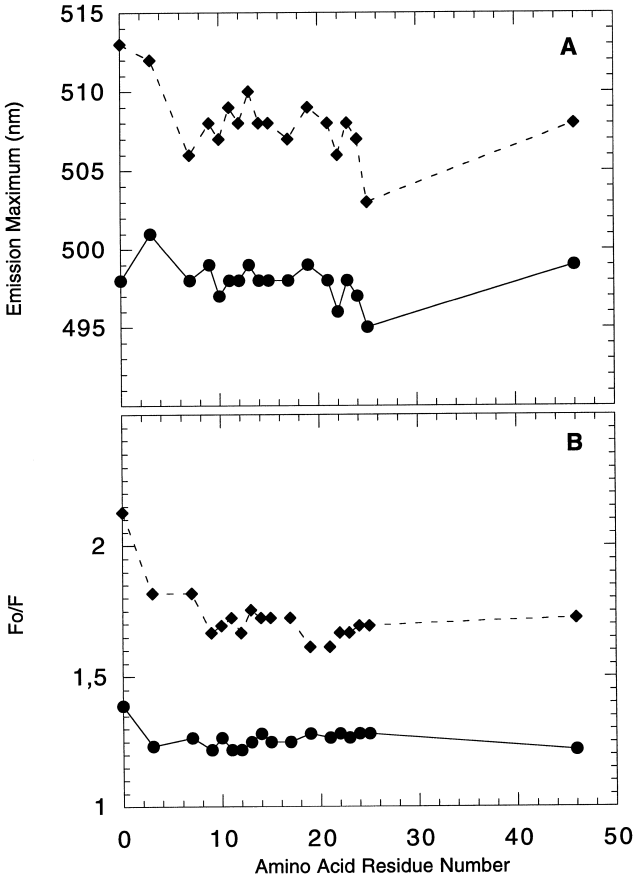

Fig. 2. Wavelengths of maximum emission (A) and acrylamide quenching efficiency profiles (B) of AEDANS attached at different positions along the primary structure the N-terminal part of the M13 coat protein when solubilized in 85% (v/v) TFE in water (solid line) and when solubilized in SDS at 50 mM final concentration (dashed line). The coat protein concentration was kept constant at 5 μM. The values at position 0 represent unbound AEDANS. The quenching efficiency is expressed as F_0/F after addition of acrylamide at a concentration of 125 mM.

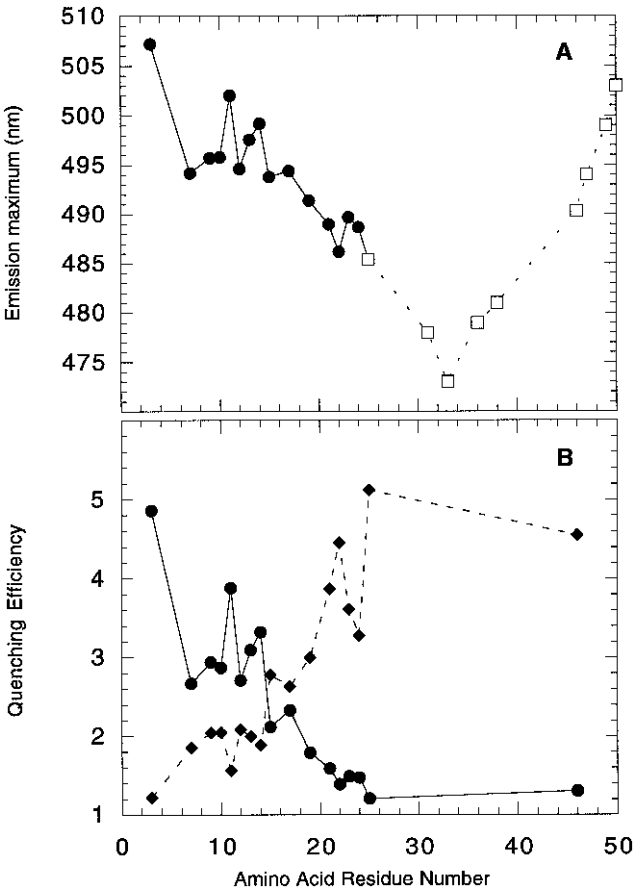

Fig. 3. Wavelengths of maximum emission of AEDANS attached to different positions along the primary structure the N-terminal part of the M13 coat protein (solid line, closed symbols) after reconstitution into DOPC/DOPG at L/P 100 (A). The values for the positions 25–50 (dashed line, open symbols) were adapted from a previous study [11]. Quenching efficiency profiles after addition of acrylamide (solid line, values expressed as K_{sv} (M^{-1})) and 5-doxyl stearic acid (dashed line, values expressed as F_0/F) are shown in B. The coat protein concentration was kept constant at 5 μM.

3.4. Localization of the N-terminal part of membrane-bound coat protein

Fig. 3A shows the wavelengths of maximum emission of the AEDANS probes, attached to different positions in the N-terminal part of membrane-bound coat proteins (residues 3–24), as well as to the previously established transmembrane and C-terminal positions 25–50 [11]. The coat protein is reconstituted into DOPC/DOPG 80%/20% (mol/mol) bilayers at L/P 100. Apart from positions 3, 11, 13 and 14, the probes attached to the N-terminal arm show wavelengths of maximum emission varying between 494 and 496 nm, which is higher as compared to the wavelength of maximum emission of AEDANS attached to the transmembrane boundary positions 25 and 46. In the case of position 3 (the outermost N-terminal position measured and not part of the amphipathic helix) a much higher wavelength (507 nm) is found, which is quite close to the value found for unbound AEDANS in aqueous buffer (512 nm). Also, the AEDANS attached to the cysteines at positions 11 (phenylalanine replacement) and 14 (leucine replacement) show remarkable high wavelengths of maximum emission of 502 and 499 nm, respectively. These latter wavelengths are about 6 nm higher than the average wavelength of maximum emission of the neighboring amino acid residues. Going from positions 17 to 25 (representing the hinge region, connecting the N-terminal and transmembrane helices), a gradual decrease of wavelength of maximum emission from 494 to 485 nm is observed. In the case of positions 23 and 24 slightly higher wavelengths are observed. Overall, these wavelengths are well below the average wavelengths of maximum emission of the N-terminal arm of the major coat protein.

For the quenching experiments both a polar but uncharged quencher molecule (acrylamide) and a hydrophobic quencher molecule (5-doxyl stearic acid) are used. The quenching results are shown in Fig. 3B as a function of different AEDANS attachment sites on the N-terminal part of the coat protein. The quenching efficiency is expressed differently for the two quenchers. In the case of acrylamide the Stern–Volmer constant K_{sv} is given, as calculated from a series of concentration-dependent experiments. However, in the case of the hydrophobic and, thus, membrane-associated quencher 5-doxyl stearic acid, the actual concentrations are unknown due to accumulation of the fatty acid in the small partial volume occupied by the bilayers interior. Therefore, F/F_0 at a constant overall quencher concentration is used instead. As observed before [11], the wavelengths of maximum emission showed again a small blue and red shift upon addition of acrylamide and 5-doxyl stearic acid, respectively.

The quenching efficiencies of acrylamide found for the N-terminal part of the protein are higher as compared to those found for the transmembrane bound-

ary positions 25 and 46. Another striking feature is the gradual decrease in quenching efficiency going from the N-terminus towards the transmembrane boundary position 25. Clearly the more N-terminal positions are better accessible to acrylamide than those closer to position 25. Similarly, as observed for the exceptional high wavelengths of maximum emission (Fig. 3A), the quenching efficiency of acrylamide on AEDANS attached to positions 3, 11, and 14 is also remarkably high.

The quenching results of the hydrophobic membrane-embedded 5-doxyl stearic acid are opposite to that of acrylamide, and a remarkable mirror resemblance is found (Fig. 3B). In this case, the lowest quenching efficiencies are obtained for the outermost N-terminal positions, and again a gradual but now increasing quenching efficiency is observed towards the transmembrane boundary position 25.

3.5. Influence of membrane-anchoring residues

Based on the typical results obtained for the coat protein labeled at position 11 (phenylalanine replacement) and position 14 (leucine replacement), these two amino acids are the subject of a further study. In addition the influence of lysine at position 8 is also examined, as lysine residues are reported to be involved in membrane anchoring as well [11,12,39]. To monitor the configuration of the N-terminal arm, the A7C coat protein mutant is selected. This labeling position is quite far away from the putative hinge between the two helical parts of the coat protein, and therefore highly sensitive for monitoring any change in protein configuration. Table 1 shows the fluorescence properties of the AEDANS labeled A7C-derived double mutants, after reconstitution into DOPC/DOPG 80%/20% (mol/mol) at L/P 100. Compared to the single A7C coat protein mutant, the additional substitutions K8A, F11A, and L14A result in higher wavelengths of maximum emission, indicative for an increased polar environment. An enhanced quenching efficiency of the polar quencher acrylamide, and a lower quenching efficiency of the hydrophobic quencher 5-doxyl stearic acid support this observation. Removal of both two hydrophobic residues phenylalanine 11 and leucine 14 results in a high emission maximum (505 nm) and a K_{sv} value for the hydrophilic quencher acrylamide of almost

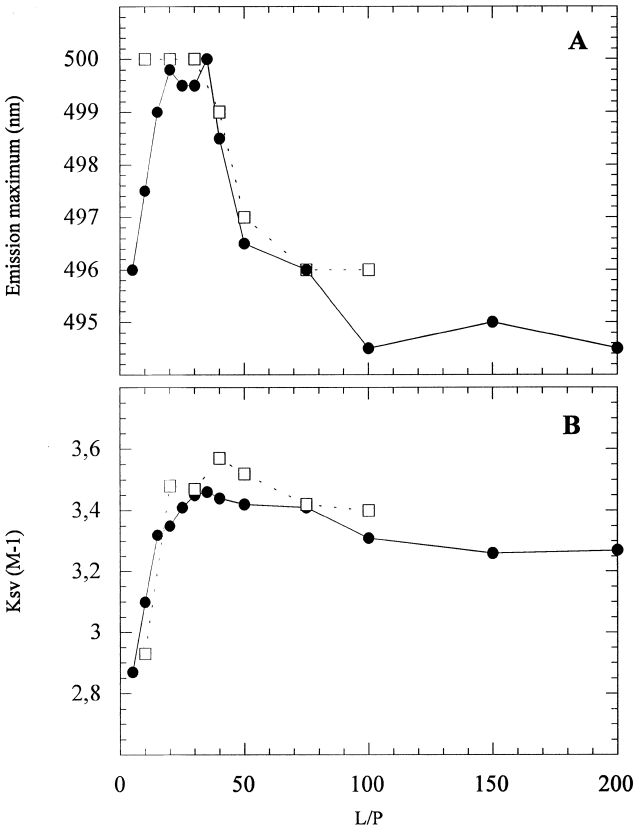

Fig. 4. Wavelengths of maximum emission (A) and acrylamide quenching profile (B) of AEDANS attached to the cysteine of M13 coat protein mutant A7C (closed circles; solid line) and of AEDANS-labeled M13 coat protein mutant A7C, which is tenfold diluted with unlabeled wild-type coat protein (open squares; dotted line), reconstituted into DOPC/DOPG at different L/P ratios. The coat protein concentration was kept constant at 2.5 μM.

6 M^{-1}. No enhanced effect was observed when the hydrophobic leucine at position 14 was replaced for the negatively charged aspartic acid (i.e., A7C/L14D). In contrast, the addition of an extra hydrophobic amino acid (A7C/A10I) results in a somewhat lower wavelength of maximum emission and concomitant quenching features.

3.6. Influence of lipid to protein ratio

The fluorescence properties of the AEDANS labeled A7C mutant, reconstituted into DOPC/DOPG 80%/20% (mol/mol) at different L/P ratios, are shown in Fig. 4. Both the wavelength of maximum emission and accessibility to the hydrophilic quencher acrylamide show maximal values around

Table 2
Quencher efficiencies and environmental polarity of the AEDANS-labeled A7C coat protein mutant in different phospholipid systems

Phospholipid composition	Emission maximum (nm)	K_{sv} (M^{-1})	Quenching by acrylamide	Quenching by 5-doxyl stearic acid F/F_0
DOPC (100%)	498	3.17		0.63
DOPC/DOPG (80%/20%)	499	3.60		0.67
DOPG (100%)	504	5.03		0.81
DOPE/DOPC (70%/30%)	500	3.61		0.66
DOPE/DOPG (70%/30%)	500	3.83		0.68
DOPE/DOPG/CL (70%/20%/10%)	500	3.83		0.67

Wavelengths of maximum emission and accessibilities to the hydrophilic quencher acrylamide and hydrophobic quencher 5-doxyl stearic acid are determined on AEDANS attached to the cysteine of M13 coat protein mutant A7C. The coat protein is reconstituted at a final concentration of 2.5 μM into DOPC/DOPG at a fixed L/P ratio of 40. The concentrations of the quencher molecules are mentioned in Section 2.

L/P 30. At L/P ratios below 30 a blue shift of the wavelength of maximum emission is observed. This blue shift is apparently a result of probe–probe interaction, since it appeared to be absent when the concentration of labeled coat protein was diluted tenfold with unlabeled wild-type coat protein (Fig. 4A). At L/P ratios below 20 lower quenching efficiencies are observed (Fig. 4B). These lower quencher accessibilities are probably due to steric hindrance at reduced protein–protein distances. The major coat protein was found to be predominantly monomeric as judged from SDS–PAGE and no higher order oligomers could be detected. At L/P ratios around L/P 20 to 35, the red-shifted wavelength of maximum emission and an increased accessibility for acrylamide both indicate a more polar environment around the N-terminal protein part.

3.7. Influence of phospholipid headgroup

The fluorescence properties of AEDANS-labeled A7C coat protein mutant in different phospholipid systems are listed in Table 2. In the case of the pure zwitterionic DOPC an emission maximum of about 498 nm is observed. Addition of negatively charged DOPG up to 20% results in a small red shift, whereas in pure negatively charged DOPG a wavelength of maximum emission of 504 nm is obtained. In analogy to previous observations, the accessibilities observed for the hydrophilic acrylamide are lower in the case of a lower wavelength of maximum emission and higher in the case of a higher wavelength of maximum emission. Again, this effect is reversed using the hydrophobic quencher 5-doxyl stearic acid. In the case of PE-containing mixtures, however, both the wavelength of maximum emission and quenching efficiencies are slightly affected.

4. Discussion

4.1. Coat protein mutant approach

In this paper we describe a new method to produce mutants of the major coat protein of bacteriophage M13. All overexpressed coat protein mutants are successfully inserted into the cytoplasmic membrane as they are subsequently processed by *E. coli* leader peptidase. This justifies a study of the membrane-bound state of these coat protein mutants. This approach opens unlimited possibilities to study the properties of the membrane-bound protein by site-specific labeling. It is now possible to study the role of individual amino acids residues throughout the whole primary sequence of the protein. In the present work, we focus on the N-terminal part of the protein. By employing fluorescence spectroscopy of AEDANS-labeled single and double mutants detailed information can be obtained about the N-terminal protein part. The double mutant approach (Table 1) comprises the monitoring of the N-terminal arm at a fixed position as a function of various supplemental X-Ala substitutions. This approach reduces a possible disturbing effect of site-specific labeling on our results. With the current state-of-the-art of mutagenesis and purification of small membrane-proteins,

a wealth of additional biophysical results may be expected in the coming years.

4.2. Fluorescence analysis

From the fluorescence experiments a clear tendency is observed: A higher value of the wavelength of maximum emission is always concomitant with an enhanced quenching efficiency of the hydrophilic acrylamide, and a lower quenching efficiency of the hydrophobic quencher 5-doxyl stearic acid. This observation indicates that environmental polarity as observed by the wavelength of maximum emission is related to accessibility as monitored predominantly by quenching. In addition, from Fig. 2 it follows that there is hardly any effect of the neighboring amino acid residues. Therefore we interpret this tendency as moving the labeled site away from the membrane surface. Because the fluorescent label as well as the N-terminal protein part may exhibit local motions, the fluorescence results will always show the average of an ensemble of conformations.

4.3. Membrane assembly of M13 coat protein

Compared to the previously established locations of the transmembrane helix boundary positions 25 and 46 [11], the amphipathic N-terminal arm is located in a more polar environment. Based on the fluorescence results in Fig. 3, the N-terminal arm is embedded along the membrane surface. This L-shaped configuration is in agreement with other studies on the M13 coat protein [16–18].

In detail, the data show a gradual decrease in wavelength and concomitant quenching efficiency going from residue 3 towards residue 19. These data can be interpreted in a structural way as a gradual entry into the membrane. Apart from the results obtained for the labeled mutant coat proteins F11C and L14C, which will be explained in the next section, it is clear that the most N-terminal labeled position 3 within the acidic amino acid block (Glu2, Asp4, Asp5) is farthest outside the net negatively-charged DOPC/DOPG membrane. This is related to the high polarity and membrane-repelling electrostatic properties of this domain, as well as to the observed high mobility features [40]. In contrast, the amino acid residues at positions 19–24, flanking the other side of the N-terminal arm and comprising the hinge region, are more buried into the membrane. The combination of these two effects results in a slight apparent tilt of the N-terminal arm with respect to the membrane surface.

In agreement with this view, a more dynamic interpretation can be used to explain the gradual changes in wavelength of maximum emission and quenching efficiencies. As the N-terminal arm of the coat protein is only loosely associated to the membrane surface (see the sections below), the N-terminal arm will be movable, and the most N-terminal positions will apparently show the lowest probability to assume a location close to the membrane surface.

4.4. Rearrangement of the N-terminal arm of the coat protein

The fluorescence results obtained for the labeled mutant coat proteins F11C and L14C indicate a location of the AEDANS probe relatively far from the membrane surface (see Fig. 3). This effect may be related to the substitution of the hydrophobic amino acids phenylalanine and leucine, respectively, by a labeled cysteine. This substitution probably affects the membrane-anchoring properties of the N-terminal protein arm. To investigate this effect more closely, double mutants were prepared based on the A7C mutant. An additional hydrophobic residue on position 10 (A7C/A10I) results in a somewhat decreased polarity surrounding the AEDANS at position 7 (see Table 1). This suggests that the N-terminal arm becomes closer to the membrane surface when it contains more hydrophobic amino acid residues. In contrast, substitution of the hydrophobic amino acid residues phenylalanine and leucine by alanine results in a substantially increased polarity (see Table 1). Similar effects are observed in the case of substitution of lysine by alanine, and by replacement of the hydrophobic leucine by the negatively charged aspartic acid. This means that, on average, the N-terminal arm probed at position 7 is located more outside the membrane. This indicates a loss of membrane-anchoring capacity and a rearrangement of the N-terminal protein part with respect to the membrane surface. From these experiments it follows that by slight modifications in the

polar-hydrophobic balance of the amphipathic N-terminal protein part, the L-shaped configuration can easily change into a more extended one, perpendicular to the membrane surface.

4.5. Phospholipid composition

Other factors that could affect the configuration of the N-terminal part of the protein may be related to the phospholipid composition of the membranes as well as the lipid to protein ratio. The phospholipid composition of the inner membrane of *E. coli* is about 70% phosphatidylethanolamine (PE), 25% phosphatidylglycerol (PG), and 5% cardiolipin [41, 42]. During the normal development of the bacteriophage M13 infection process, the phospholipid composition of the inner membrane is little affected in favor of the charged phospholipids PG and especially CL [43–45]. It has been shown that accumulation of high amounts of the major coat protein in the inner membrane result in significantly increased levels of CL and PG, and a compensating decline in PE [41,43,45]. This strongly suggests a role of CL and PG in conserving the functional state of the membrane-bound coat protein. The effect of the composition of the model membranes used in our experiments is shown in Table 2. From this table it is clear that the influence of the phospholipid headgroup composition on the fluorescence results is small. This result indicates that within the range thought to be relevant in vivo, the membrane composition can be excluded as a direct factor in the structural rearrangement of the N-terminal arm.

4.6. Space-limiting effects

Local accumulation of major coat proteins possibly may create a lack of space at the membrane surface. It can easily be imagined that the N-terminal part of the protein partially embedded in the phospholipid headgroup region will occupy more space in the membrane as compared to an extended configuration. Experimentally, the position of the N-terminal protein part can be forced to adapt just by varying the lipid to protein ratio. As shown in Fig. 4, a more polar environment and increased quenching efficiency of acrylamide can be seen around L/P 20–35. This effect can be explained by assuming that the N-terminal arm moves away from the membrane surface. From these results we conclude that effects related to membrane-anchoring and space-limiting effects are key factors for the structural rearrangement of the N-terminal arm of the membrane-bound major coat protein.

4.7. Conclusions

In previous structural views of the membrane-bound state of the M13 coat protein, the protein is in an L-shape in which the N-terminal arm is embedded along the membrane surface [16–18]. In the present work, it is demonstrated that the N-terminal arm can exist in an L-shape as well as in a more extended I-shape. The N-terminal arm of the membrane-associated coat protein is not just firmly fixed to the membrane and can move off the membrane surface and into solution. Apparently, there is no tight association of the N-terminal arm to the membrane surface. This structural modulation may have consequences for the protein in its role in the assembly process of the phage. During assembly the proteins must come together in the membrane. This requires a close approach of the transmembrane domains of the coat protein, which may be hindered by steric effects of the protein in the L-shape. However, as the N-terminal arm of the membrane-bound protein is loosely associated to the membrane, it can easily adapt to a more extended I-shape. In this state, the protein also has the proper configuration to form the viral coat, enabling fast and efficient phage assembly.

References

[1] P. Model, M. Russel, in: R. Calendar (Ed.), The Bacteriophages, vol. 2, Plenum, New York, 1988, pp. 375–456.
[2] M. Russel, Trends Microbiol. 3 (1995) 223–228.
[3] R.E. Webster, in: B.K. Kay, J. Winter, J. McCafferty (Eds.), Phage Display of Peptides and Proteins, Academic Press, New York, 1996, pp. 1–20.
[4] D.A. Marvin, Curr. Opin. Struct. Biol. 8 (1998) 150–158.
[5] R.B. Spruijt, M.A. Hemminga, Biochemistry 30 (1991) 11147–11154.
[6] Z.M. Li, M. Glibowicka, C. Joensson, C.M. Deber, J. Biol. Chem. 268 (1993) 4584–4587.
[7] D. Stopar, R.B. Spruijt, C.J.A.M. Wolfs, M.A. Hemminga, Biochemistry 36 (1997) 12268–12275.

[8] N.G. Haigh, R.E. Webster, J. Mol. Biol. 279 (1998) 19–29.
[9] F.C.L. Almeida, S.J. Opella, J. Mol. Biol. 270 (1997) 481–495.
[10] C.H.M. Papavoine, B.E.C. Christiaans, R.H.A. Folmer, R.N.H. Konings, C.W. Hilbers, J. Mol. Biol. 282 (1998) 401–419.
[11] R.B. Spruijt, C.J.A.M. Wolfs, J.W.G. Verver, M.A. Hemminga, Biochemistry 35 (1996) 10383–10391.
[12] D. Stopar, R.B. Spruijt, C.J.A.M. Wolfs, M.A. Hemminga, Biochemistry 35 (1996) 15467–15473.
[13] J. Kyte, R.F. Doolittle, J. Mol. Biol. 157 (1982) 105–132.
[14] R.J. Turner, J.H. Weiner, Biochim. Biophys. Acta 1202 (1993) 161–168.
[15] C.H.M. Papavoine, M.L. Remerowski, L.M. Horstink, R.N.H. Konings, C.W. Hilbers, F.J.M. van de Ven, Biochemistry 36 (1997) 4015–4026.
[16] P.A. Mcdonnell, K. Shon, K. Kim, S.J. Opella, J. Mol. Biol. 233 (1993) 447–463.
[17] F.M. Marassi, A. Ramamoorthy, S.J. Opella, Proc. Natl. Acad. Sci. USA 94 (1997) 8551–8556.
[18] W.F. Wolkers, R.B. Spruijt, A. Kaan, R.N.H. Konings, M.A. Hemminga, Biochim. Biophys. Acta 1327 (1997) 5–16.
[19] D.A. Marvin, R.D. Hale, C. Nave, M.H. Citterich, J. Mol. Biol. 235 (1994) 260–286.
[20] W.M. Tan, R. Jelinek, S.J. Opella, P. Malik, D.T. Tamsin, R.N. Perham, J. Mol. Biol. 286 (1999) 787–796.
[21] A.B. Meijer, R.B. Spruijt, C.J.A.M. Wolfs, M.A. Hemminga, Biochemistry 39 (2000) 6157–6163.
[22] S.L. Flitsch, H.G. Khorana, Biochemistry 28 (1989) 7800–7805.
[23] J.H. Lakey, D. Baty, F. Pattus, J. Mol. Biol. 218 (1991) 639–653.
[24] P.C. Jones, A. Sivaprasadarao, D. Wray, J.B.C. Findlay, Mol. Membr. Biol. 13 (1996) 53–60.
[25] E.N. Hudson, G. Weber, Biochemistry 12 (1973) 4154–4161.
[26] M.R. Eftink, C.A. Ghiron, Anal. Chem. 114 (1981) 199–227.
[27] P.M.G.F. Van Wezenbeek, T.J.M. Hulsebos, J.G.G. Schoenmakers, Gene 11 (1980) 129–148.
[28] S. Tabor, in: F.A. Ausubel, R. Brent, R.E. Kingston, D.D. Moore, J.G. Seidman, J.A. Smith, K. Struhl (Eds.), Current Protocols in Molecular Biology, Greene Publishing and Wiley-Interscience, New York, 1990, pp. 16.2.1–16.2.11.
[29] F.W. Studier, A.H. Rosenberg, J.J. Dunn, J.W. Dubendorf, Methods Enzymol. 185 (1990) 60–89.
[30] H. Schägger, G. Von Jagow, Anal. Biochem. 166 (1987) 368–379.
[31] J. Sambrook, E.F. Fritsch, T. Maniatis, Molecular Cloning: A Laboratory Manual, Cold Spring Harbor Laboratory Press, Cold Spring Harbor, NY, 1989.
[32] R.B. Spruijt, C.J.A.M. Wolfs, M.A. Hemminga, Biochemistry 28 (1989) 9158–9165.
[33] H. Endemann, P. Model, J. Mol. Biol. 250 (1995) 496–506.
[34] A. Kuhn, W. Wickner, J. Biol. Chem. 260 (1985) 15907–15913.
[35] M. Russel, B. Kazmierczak, J. Bacteriol. 175 (1993) 3998–4007.
[36] D.C. LaPorte, C.H. Keller, B.B. Olwin, D.R. Storm, Biochemistry 20 (1981) 3965–3972.
[37] S.S. Lehrer, P.C. Leavis, Methods Enzymol. 49 (1978) 222–236.
[38] K. Mandal, B. Chakrabarti, Biochemistry 27 (1988) 4564–4571.
[39] J. Ren, S. Lew, Z. Wang, E. London, Biochemistry 36 (1997) 10213–10220.
[40] M.J. Bogusky, G.C. Leo, S.J. Opella, Proteins Struct. Funct. Genet. 4 (1988) 123–130.
[41] J.L. Woolford Jr., J.S. Cashman, R.E. Webster, Virology 58 (1974) 544–560.
[42] E. Burnell, L. Van Alphen, A. Verkleij, B. De Kruijff, Biochim. Biophys. Acta 597 (1980) 492–501.
[43] Y. Ohnishi, J. Bacteriol. 107 (1971) 918–925.
[44] B.K. Chamberlain, R.E. Webster, J. Biol. Chem. 215 (1976) 7739–7745.
[45] G. Pluschke, Y. Hirota, P. Overath, J. Biol. Chem. 253 (1978) 5048–5055.